Available online at www.eccomasproceedia.org
Eccomas Proceedia COMPDYN (2021) 84-101

ECCOMAS
Proceedia

COMPDYN 2021
8th ECCOMAS Thematic Conference on
Computational Methods in Structural Dynamics and Earthquake Engineering
M. Papadrakakis, M. Fragiadakis (eds.)
Streamed from Athens, Greece, 28 - 30 June 2021

EFFECT OF IN-PLANE/OUT-OF-PLANE INTERACTION IN INFILL WALLS ON THE FLOOR SPECTRA OF REINFORCED CONCRETE BUILDINGS

Mariano Di Domenico[1], Paolo Ricci[1], and Gerardo M. Verderame[1]

[1] Department of Structures for Engineering and Architecture, University of Naples Federico II
Via Claudio 21 – 80125 – Naples, Italy
e-mail: {mariano.didomenico, paolo.ricci, verderam}@unina.it

Abstract

Currently, in the framework of performance-based earthquake engineering, the seismic assessment of buildings should be performed by considering the safety of non-structural components. This is necessary to protect human life safety from their collapse, as well as to limit the economic losses associated with their damage. Typically, the safety assessment of non-structural components is performed with a force-based approach, i.e., by comparing their force/acceleration capacity with the expected force/acceleration demand under the design earthquake scenario, i.e., with reference to different limit states.
Different acceleration demand models, i.e., floor response spectra, exist, but relatively few of them were defined by considering the influence on the structural response of the in-plane response of infill walls, and none of them by considering the so-called "in-plane/out-of-plane interaction" effects. In other words, it is nowadays well known that the out-of-plane damage of unreinforced masonry infills affects their in-plane response, thus influencing the seismic response (and the floor response spectra) of the supporting structure.
In this paper, non-linear time-history analyses are performed on reinforced concrete framed buildings with different number of storeys, design level, and infill wall layout. The analyses are performed on the bare structure as well as on the infilled structure by considering and by not considering the in-plane/out-of-plane interaction effects in the infill wall model. The acceleration floor spectra derived from the analyses are compared, thus investigating the potential effect of the in-plane/out-of-plane interaction effect on the expected acceleration demand acting on infill walls.

Keywords: RC structure, infill wall, out-of-plane, seismic assessment, floor spectrum.

ISSN:2623-3347
Peer-review under responsibility of the organizing committee of COMPDYN 2021.
doi: 10.7712/120121.8464.19313

1 INTRODUCTION

In the framework of performance-based earthquake engineering, the seismic assessment of nonstructural components is a paramount issue: in fact, most of the earthquake-induced damage to buildings and the consequent economic losses is related to the response of nonstructural elements. Nonetheless, the heavy damage of certain nonstructural components, such as infill walls, may even threaten human life safety. For these reasons, there is need for the development of robust and reliable models for the assessment of capacity and demand associated with nonstructural elements. This work is focused on the definition of the acceleration demand acting on them, i.e., on floor response spectra.

Floor response spectra are a useful tool for the assessment of the pseudo-acceleration demand acting on acceleration-sensitive nonstructural components within a linear force-based approach, which is typical of the design process of new buildings. To understand what a floor spectrum is, the simplest way is considering the usual approach to the seismic analysis of a building. It is well-known that a structure subjected to a certain earthquake, i.e., to a certain ground motion acceleration time-history, will experience a certain maximum acceleration demand which is different from the maximum acceleration demand at its base, which is also known as Peak Ground Acceleration (PGA). This occurs since the ground motion is filtered by the structure through its mass, deformability and damping properties, thus resulting in an acceleration response history of the structure different from that applied to the base and in a maximum pseudo-acceleration demand named pseudo-spectral acceleration (S_a) different from PGA. The S_a acting on a certain structure represented by an equivalent Single Degree of Freedom (SDOF) system characterized by vibration period T and damping ratio ξ can be simply calculated through the pseudo-acceleration response spectrum of the ground motion. Similarly, the maximum pseudo-spectral acceleration, herein identified as PSA, acting on a nonstructural component represented by an SDOF system with vibration period T_a and damping ratio ξ_a supported by a certain floor of a structure can be calculated through the pseudo-acceleration response spectrum of the acceleration time-history of the supporting floor. This pseudo-acceleration response spectrum is known as floor response spectrum.

In other words, a stiff nonstructural component (i.e., a nonstructural component with T_a=0) attached to a certain floor of a structure will experience a PSA equal to the maximum acceleration demand of that floor, which is named Peak Floor Acceleration (PFA) and is different from the PGA. If T_a is higher than zero, the PSA will be different from the PFA dependently on T_a and ξ_a. These concepts are summarized in Figure 1.

So, based on the above discussion, the seismic demand acting on a certain nonstructural component supported by a certain floor of the structure can be known if the PFA of that floor and the floor spectral shape are known. In addition, based on the above discussion, it is possible to define some parameters that, intuitively, are expected to have an influence on the PFA and on the spectral shape. Regarding the PFA, one can expect its dependence on the PGA value (the higher the PGA, the higher the PFA) and on the height of the specific floor considered, z, potentially normalized with respect to the total building height, H. Regarding the spectral shape, one can expect that the PSA is amplified or de-amplified with respect to the PFA, with the maximum amplification expected due to resonance of the nonstructural component and of the structure, i.e., when T_a is closer to the fundamental vibration period(s) of the supporting structure. As will be shown later in this paper, further parameters may have a paramount influence on both the PFA distribution along the building height and the floor spectral shape.

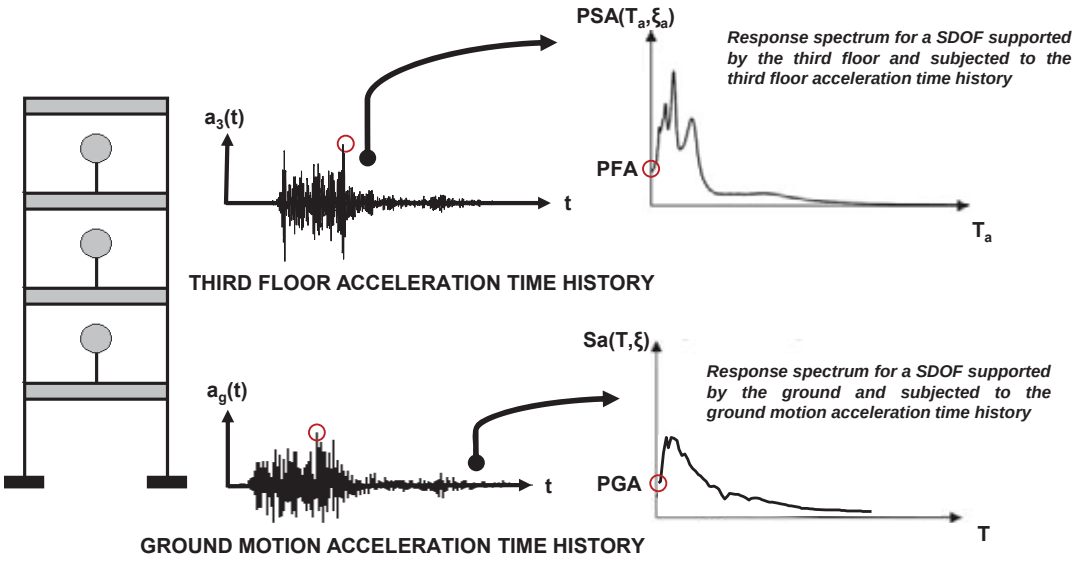

Figure 1: Concept of floor response spectrum.

In this study, the state-of-the-art of current code and literature formulations is presented, mainly to define a systematic review of the geometric and mechanical structural parameters which are expected to influence the PFA distribution along the building height and the floor spectral shape. Second, nonlinear models of bare and infilled case-study reinforced concrete framed buildings with 2, 4, 6 and 8 storeys designed for different PGA levels (0.05 g, 0.15 g, 0.25 g and 0.35 g) according to Eurocodes are defined. Then, nonlinear time history analyses are performed on the case-study buildings to evaluate floor response spectra. The numerical outcomes are compared in order to analyze the effect of the presence of infill walls on floor response spectra considering and not considering the out-of-plane response of infill walls and the mutual interaction between their in-plane and out-of-plane response (i.e., the in-plane/out-of-plane interaction). To this aim, a recent out-of-plane and in-plane/out-of-plane interaction model proposed by the Authors of this study is updated in order to account for the potential softening and cyclic degradation of the out-of-plane response of infill walls. Note that modelling the out-of-plane response of infills and the in-plane/out-of-plane interaction is a novelty element for studies dedicated to floor spectra assessment, which rarely have been dedicated to infilled buildings in general.

2 SUMMARY OF EXISTING FORMULATIONS

Several studies have been dedicated to floor response spectra in past and recent times. Comprehensive state-of-the-art reviews are proposed by Rodriguez et al. [1] and by Vukobratović [2]. In this section, for the sake of conciseness, the discussion is focused on recent practice-oriented proposals available in the literature, as well as on main code prescriptions regarding this topic.

2.1 Code proposals

Eurocode 8 [3], in section 4.3.5, proposes an expression for the PSA as shown, with some manipulation in the nomenclature, in Equation 1.

$$PSA = PGA\left[\frac{3(1+z/H)}{1+(1-T_a/T_1)^2}-0.5\right] \quad (1)$$

In Equation 1, T_a is the non-structural element vibration period and T_1 is the fundamental vibration period of the structure. If T_a equals zero, a linear PFA distribution along the building height is obtained at varying z/H ratio. PFA ranges from PGA (at z equal to zero) to 2.5PGA (at z equal to H). On the other hand, the maximum PSA is obtained if T_a equals T_1. In this case, the maximum PSA ranges from 2.5PGA (at z equal to zero) to 5.5PGA (at z equal to H). It should be noted that this formulation returns a maximum PSA/PFA ratio different for each floor. This will be observed also from the numerical analyses performed in this study.

ASCE/SEI 7-10 [4], in section 13.3.1, proposes an expression for the PSA as shown, with some manipulation in the nomenclature, in Equation 2.

$$PSA = PGA\left(1 + 2\frac{z}{H}\right)a_p \tag{2}$$

In Equation 2, a_p is a factor accounting for the amplification of accelerations due to the deformability of the non-structural element reported in Table 13.5-1 of the code. It is worth noting that the American approach, with this factor, simplifies the calculation of the seismic demand acting on non-structural elements, as there is no need of a more or less detailed dynamic characterization of the nonstructural element required for the determination of its period, T_a, which enters Eurocode 8 [3] formulation. Exterior non-structural wall elements, such as unreinforced masonry infills, are associated with an a_p factor equal to 1.00.

Also according to the ASCE/SEI 7-10 [4] approach, the PFA varies linearly along the building height. It ranges from PGA (at z equal to zero) to 3PGA (at z equal to H). The maximum value of a_p reported in Table 13.5-1 of the code is equal to 2.5. Hence, the maximum possible PSA value is always equal to 2.5PFA, independently on the floor considered.

The New Zealand code NZSEE2017 [5], in section C7.6.2, refers to the loading code NZS 1170.5 [6] for the calculation of floor response spectra. NZS 1170.5 [6], in section 8.5.1, provides the formulation reported, with some manipulation in the nomenclature, in Equation 3 to calculate the PSA.

$$PSA = PGAC_{Hi}C_i(T_a) \tag{3}$$

C_{Hi} is calculated through the formulations reported in Equation 4 and defines the PFA distribution along the building height which is, in this case, multilinear. The PFA ranges from PGA (at z equal to zero) to 3PGA (at z equal to H).

$$C_{Hi} = \left(1 + \frac{z}{6}\right) \qquad \text{for all z<12 m} \tag{4a}$$

$$C_{Hi} = \left(1 + 10\frac{z}{H}\right) \qquad \text{for z<0.2H} \tag{4b}$$

$$C_{Hi} = 3.0 \qquad \text{for z}\geq\text{0.2H} \tag{4c}$$

In Equation 3, $C_i(T_a)$ is the spectral shape coefficient. $C_i(T_a)$ is expressed as a function of the period T_a and ranges from 0.5 for T_a higher than 1.50 s to 2.0 for T_a lower than 0.75 s. Hence, the maximum possible PSA value is always equal to 2PFA, independently on the floor considered. It is worth noting that, in this case, the maximum PSA value depends on the "absolute" value of T_a, i.e., it does not depend on T_a/T_1 ratio.

As above shown, the previous code prescriptions generally relate the PFA linear or multilinear distribution along the building height to the floor height normalized with respect to the building height (i.e., the higher z/H, the higher the PFA) and the PSA spectral shape to the ratio between the T_a and T_1. From both these features, it can be assumed that they relate the floor response spectra to the elastic response of the structure to its first vibration mode.

The commentary (Circolare 2019, [7]) to the current Italian building code (NTC2018, [8]) defines a "rigorous" approach for the assessment of floor response spectra as well a simplified approach specific for framed reinforced concrete structures. Both account for multi-modal contributions and for the effect on floor response spectra of structural nonlinearity. In fact, structural nonlinearity limits the maximum force acting on a structure: hence, it also may limit the maximum acceleration acting at its floors. Both topics have been also highlighted in recent literature, as will be shown in the next subsection.

The rigorous approach accounts for multi-modal contributions based on simple considerations related to structural dynamics. In fact, the PFA_{ij} acting at the j-th floor of the structure associated with its i-th vibration mode is determined by means of Equation 5.

$$PFA_{ij} = \Gamma_i \varphi_{ij} S_a(T_i) \tag{5}$$

In Equation 5, Γ_i is the modal participation factor of the i-th vibration mode, φ_{ij} is the modal displacement of the j-th storey for the i-th vibration mode, $S_a(T_i)$ is the spectral acceleration of the structure associated with its i-th vibration period, potentially reduced by means of the structure behaviour factor. The PSA is obtained, for each floor and for each vibration mode contribution, by amplifying or de-amplifying the PFA through an R factor (which equals PSA_{ij}/PFA_{ij}) calculated by means of Equation 6.

$$R_{ij} = \frac{PSA_{ij}}{PFA_{ij}} = \left(\sqrt{\left(2\xi_a \frac{T_a}{T_i}\right)^2 + \left(1 - \frac{T_a}{T_i}\right)^2} \right)^{-1} \tag{6}$$

Equation 6 returns a PSA_{ij} value equal to $1/2\xi_a$ times PFA_{ij} for $T_a=T_i$. The value of the maximum amplification is a classical result of the dynamic of the damped SDOF system (Chopra [9]). For each storey, the floor spectrum can be obtained by combining multi-modal contributions through the SRSS rule, thus resulting in a spectral shape with multiple peaks corresponding to the number of significant modes considered. Implicitly, also the PFA at the j-th floor can be obtained through the SRSS combination of the different modal contributions, thus resulting in a potentially non-monotonic distribution along the building height. Both circumstances will be observed also from the analyses results presented in this study.

Regarding the PFA distribution, it is worth noting that Equation 6 may yield to a de-amplification of the PFA with respect to the PGA value, especially in bottom floors of high-rise structures. This circumstance has been observed by some authors (e.g., Rodriguez et al. [1], Petrone et al. [10], Surana et al. [11]), especially when analyzing elastic models, but not by other authors and never in the analyses performed in this study. A comment to this issue will be given in the next subsection, when describing the approach proposed by Calvi and Sullivan [12].

The simplified approach proposed by the Italian regulation for framed reinforced concrete structures is borrowed by the work by Petrone et al [10]. Since this proposal is based on numerical analyses on nonlinear models of reinforced concrete framed structures, it implicitly account

for both multi-modal contributions and structural nonlinearity effect. The proposed formulations are reported, with some manipulation in the nomenclature, in Equation 7.

$$PSA = \begin{cases} PGA\left(1+\frac{z}{H}\right)\left[\frac{a_p}{1+\left(a_p-1\right)\left(1-\frac{T_a}{aT_1}\right)^2}\right] \geq PGA & for\ T_a < aT_1 \\ PGA\left(1+\frac{z}{H}\right)a_p & for\ aT_1 \leq T_a < bT_1 \\ PGA\left(1+\frac{z}{H}\right)\left[\frac{a_p}{1+\left(a_p-1\right)\left(1-\frac{T_a}{bT_1}\right)^2}\right] \geq PGA & for\ T_a \geq bT_1 \end{cases} \quad (7)$$

In Equation 7, a, b, and a_p are coefficients depending on T_1 that account for higher modes effects (a), resonance period elongation due to nonlinearity (b) and effect of nonlinearity of the maximum PSA value (a_p). If T_a equals zero, a linear PFA distribution along the building height is obtained. PFA ranges from PGA (at z equal to zero) to 2PGA (at z equal to H). On the other hand, the maximum PSA is obtained if T_a is between aT_1 and bT_1. In this case, the floor spectral acceleration ranges from 2.5PFA to 5PFA, dependently on a_p value.

It is worth noting that none of the proposals discussed in this subsection explicitly refers to infilled buildings, as if the presence of infills may be considered only through T_1 value, i.e., as if the presence of infills only affects the resonance period at which the maximum PSA is attained, except for the simplified proposal of the Italian regulation, in which also the maximum PSA value depends on T_1 and attains it maximum potential value for small values of the period (i.e., a_p=5 when T_1 is lower than 0.5 s). In other words, based on this approach, an infilled building is expected to experience an equal or higher maximum PSA value, at a certain floor, with respect to an identical but bare structure. This is also generally observed in the numerical analyses shown in this paper.

2.2 Literature formulations

Calvi and Sullivan [12] propose an approach for the assessment of floor response spectra for SDOF systems extended to Multi-Degree of Freedom systems and validated against the results of numerical time-history analyses on reinforced concrete wall structures. The PSA value for each floor and for each modal contribution is calculated by means of Equation 8.

$$PSA_{ij} = \Gamma_i \varphi_{ij} a_{m,i} \quad (8)$$

In Equation 8, $a_{m,i}$ is a spectral shape function given by Equation 9.

$$a_{m,i}(T_a) = \begin{cases} \frac{T_a}{T_i}\left[a_{max,i}(DAF_{max}-1)+a_{max,i}\right] & for\ T_a < T_i \\ a_{max,i}DAF_{max} & for\ T_i \leq T_a < T_{i,eff} \\ a_{max,i}DAF_i & for\ T_a \geq T_{i,eff} \end{cases} \quad (9)$$

In Equation 9, $a_{max,i}$ is the minimum between $S_a(T_i)$ and the S_a corresponding to global yielding of the structure (S_{ay}, potentially determined by means of a nonlinear static analysis), DAF is given by Equation 10, with DAF_{max} obtained for $T_a=T_{i,eff}$.

$$DAF_i = \left(\sqrt{\left(1 - \frac{T_a}{T_{i,eff}}\right)^2 + \xi_a} \right)^{-1} \tag{10}$$

In Equations 9 and 10, $T_{i,eff}$ is the effective period of the structure (which is assumed potentially different from the elastic vibration period only for the first vibration mode), potentially evaluated through a nonlinear static analysis.

This approach accounts for the effect of multiple vibration modes contributions, which can be combined through the SRSS rule. Also, it accounts for structural nonlinearity effects in terms of resonance period elongation and limitation of the maximum PSA. Also in this case, as highlighted when discussing the Italian regulation "rigorous" approach, the PFA value may result lower than PGA. Since this is only seldom observed as a result of numerical analyses, due to, according to Calvi and Sullivan [12], the interaction between the ground motion typical frequency content and the structure dynamic properties, they suggest that the PFA value should never be assumed lower than PGA at bottom floors and that, at the same floors, the floor response spectrum should never return PSA values lower than those associated with the ground motion response spectrum.

Vukobratović and Fajfar [13, 14] propose a theoretical-based (except for the determination of the maximum PSA value, which is empirical) approach for the assessment of floor response spectra validated against the results of numerical time-history analyses on reinforced concrete frames. The PSA value for each floor and for each modal contribution is calculated by means of Equation 11.

$$PSA_{ij} = \frac{\Gamma_i \varphi_{ij}}{\left| \left(\frac{T_a}{T_{i,eff}}\right)^2 - 1 \right|} \sqrt{\left(\frac{S_a(T_{i,eff})}{R_{\mu,i}}\right)^2 + \left(\left(\frac{T_a}{T_{i,eff}}\right)^2 S_a(T_a)\right)^2} \leq AMP_i \Gamma_i \varphi_{ij} \frac{S_a(T_{i,eff})}{R_{\mu,i}} \tag{11}$$

In Equation 11, $T_{i,eff}$ is different from the elastic period only for the first vibration mode and can be calculated by means of a nonlinear static analysis; $R_{\mu,i}$ is the reduction factor due to the nonlinear behaviour of the structure and is equal to the maximum between 1 and the ratio between $S_a(T_{1,eff})$ and S_{ay} (potentially determined by means of a nonlinear static analysis) for the first vibration mode, while it is equal to 1 for higher vibration modes; AMP_i is the maximum PSA_{ij}/PFA_{ij} value and is expressed as a function of the damping ratio similarly to the approach proposed by Calvi and Sullivan [12]. The effects of multiple modes are combined by applying ALGSUM combination rule in the post-resonance region, with the SRSS rule otherwise.

3 DESIGN AND MODELLING OF THE CASE-STUDY STRUCTURES

The 2-, 4-, 6-, and 8-storey case-study reinforced concrete moment resisting frames have regular rectangular plan defined by five and three bays in the longitudinal and transverse direction, respectively. Beams are 4.5 m long; columns are 3.0 m high. The buildings were designed according to Eurocode 2 [15] and Eurocode 8 [3] for four different design PGA values at Life Safety Limit State (0.05 g, 0.15 g, 0.25 g and 0.35 g) in "High" Ductility Class (DCH). The materials used for design are class C28/35 concrete with characteristic compressive strength of

the cylinder equal to 28 N/mm^2 and steel rebars with characteristic yielding stress equal to 450 N/mm^2. It is assumed that floor slabs have a diaphragmatic behaviour. During the design and the analysis process, second-order geometric effects are neglected. Further details on the design of the case-study RC frames are available in Di Domenico [16] and in Ricci et al. [17]. For the analyses, the reinforced concrete elements' non-linearity is modelled by adopting a lumped-plasticity approach in OpenSees [18] by using ModIMKPeakOriented Material with response parameters determined according to Haselton et al. [19] and with the introduction of the cracking point. In the modelling process, average material properties are used, namely a compressive strength for concrete equal to 36 N/mm^2 determined according to Eurocode 2 [15], and a steel yielding stress equal to 517.5 N/mm^2 determined according to Fardis et al. [20].

Two different unreinforced masonry infill layouts are considered. The first is constituted by a two-leaf (thickness: 80+120 mm) 'weak' infill wall (weak layout, WL), the second is constituted by a one-leaf (thickness: 300 mm) 'strong' infill wall (strong layout, SL). Note that the two-leaf infills are constituted by independent non-interacting panels. In other words, the in-plane and the out-of-plane responses of each leaf are determined (and modelled) independently on those associated with the other leaf.

The mechanical properties of these infills are those calculated for the masonry wallets tested by Calvi and Bolognini [21] for the WL and those by Guidi et al. [22] for the SL. Each infill leaf is introduced in the structural model by using a couple of equivalent no-tension struts.

The in-plane non-linear behaviour is modelled, separately for each leaf, based on the proposal by Panagiotakos and Fardis [23]. According to this modelling approach, only the slope of the softening branch of the force-displacement in-plane behaviour relationship is an open parameter, and it should be set to a fraction α of the infill initial elastic stiffness. In Fardis [24] it is suggested to set α to a value between -1.5% and -5%. For the 80-, 120-mm thick leaves α is set to -1.6% while for the 300-mm thick leaf it is set to -3.6% in order to reproduce the experimental evidences shown by Calvi and Bolognini [21] and by Guidi et al. [22]. The two layouts analyzed are characterized by similar elastic in-plane stiffness but by different in-plane and out-of-plane strength capacity. In other words, buildings with WL and SL infills have similar elastic period, but those with WL infills are more likely to experience nonlinearity due to infills' cracking.

Regarding the out-of-plane response, the modelling strategy proposed by Ricci et al. [25] is adopted in order to account for the in-plane/out-of-plane interaction effects, i.e., the degradation of the out-of-plane strength and stiffness due to in-plane damage and of the in-plane strength and stiffness due to out-of-plane damage. The equations adopted for modelling the out-of-plane response are those proposed in Ricci et al. [17] for infills in which the out-of-plane response is governed by two-way arching effect strength mechanism, except for those associated with some response parameters. In fact, for this study, the out-of-plane response model is improved and updated.

First, the empirical equation for the assessment of the out-of-plane first macro-cracking force, F_{crack}, is updated to account for recent experimental evidences proposed by De Risi et al. [26] and by Di Domenico et al. [27] The new formulation is reported in Equation 12.

$$F_{crack} = 5.90 {f_{mv}}^{0.11} \frac{t^{0.83}}{h^{1.44}} wh \tag{12}$$

In Equation 12, forces are expressed in Newtons and lengths are expressed in millimeters. In addition, the formulations proposed by Di Domenico et al. [27] are used to model the in-plane/out-of-plane interaction effects. In these formulations, the reduction of the out-of-plane strength and stiffness capacity is related not only to the in-plane interstorey drift ratio demand

and to the infill wall vertical slenderness (i.e., the h/t ratio), but also to the infill wall aspect ratio w/h.

However, the most important and significant improvement of the out-of-plane response model is the introduction of the softening branch in the out-of-plane response backbone, as shown in Figure 2a, and the assessment of the cyclic degradation of the response envelope. As shown in Figure 2a, the out-of-plane response backbone adopted in Ricci et al. [17] was trilinear with a plastic branch after the peak load point up to the attainment of the displacement, equal to 0.30 times the infill thickness, corresponding, on average and based on experimental tests, to the 20% degradation of the maximum out-of-plane strength, which is a usual threshold associated with conventional collapse of structural members. In this study, the "conventional" ultimate point is retained at a displacement equal to 0.30 times the infill thickness. However, a bilinear softening branch is modelled. The first part of the softening branch goes from the peak load point to the "conventional" ultimate point set at a force equal to 80% of the predicted maximum strength capacity. The second part goes from the "conventional" ultimate point to the "collapse displacement" point corresponding to zero out-of-plane strength capacity, i.e., at vanishing of arching action strength mechanism. As demonstrated in Angel et al. [28] and furtherly explained in Di Domenico et al. [29], vanishing of both vertical and horizontal arching effect is expected, based on geometrical considerations, at an out-of-plane central displacement of the infill wall equal to 0.80 times the infill thickness. So, the out-of-plane collapse displacement is set, in this study, to this value.

The quadri-linear response envelope shown in Figure 2a is modelled in OpenSees [18] by adopting Pinching4 Material. Pinching4 Material also allows modelling the hysteretic degradation of strength, unloading and reloading stiffness, as well as the so-called "pinching" effect. Further details on the nature and meaning of the hysteretic parameters governing Pinching4 Material response are available in Lowes at al. [30]. A preliminary calibration of these parameters has been performed by carrying out at the laboratory of the Department of Structures for Engineering and Architecture of University of Naples Federico II (DIST-UNINA) a cyclic out-of-plane test on an unreinforced masonry infill with thickness equal to 120 mm and poor mechanical properties (i.e., nominally identical to those monotonically tested in Di Domenico et al., [31]), whose out-of-plane force (F_{OOP})-displacement (d_{OOP}) response is shown in Figure 2b. Further details on this experimental test are available in [16].

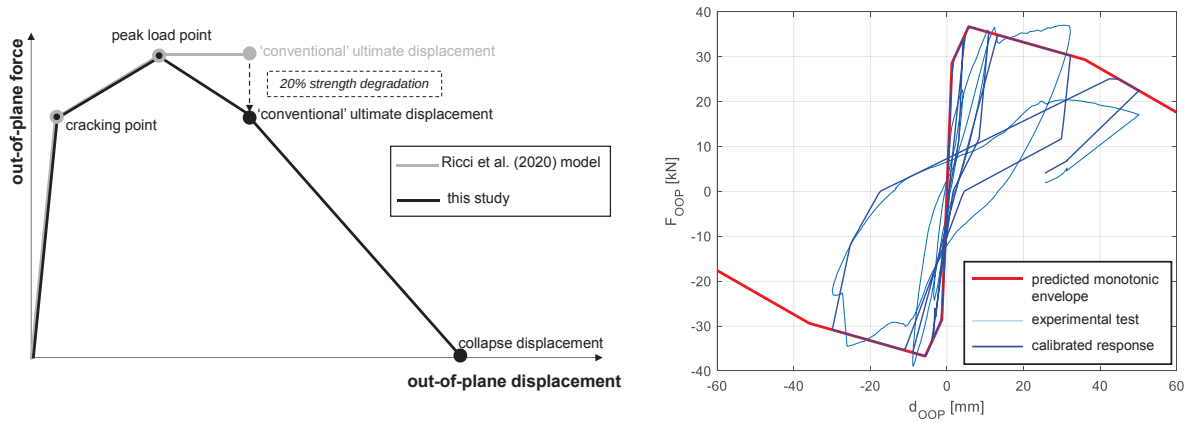

Figure 2: Updating of the out-of-plane response model: (a) new response envelope and (b) calibration of Pinching4 Material hysteretic parameters based on the cyclic test performed at DIST-UNINA.

The Pinching4 Material hysteretic parameters have been calibrated by setting damage degradation type to "energy" and in order to minimize the distance between the experimental and the predicted energy dissipation history during the entire experimental test. They have been calibrated by neglecting the force cyclic degradation, since the limited number of comparisons between monotonic and cyclic experimental tests available (e.g., [16, 32]) shows that no significant strength degradation is observed when comparing monotonic and cyclic out-of-plane tests. The calibrated parameters are gK1=2.00, gK2=0.55; gK3=1.50; gK4=0; gD1=0.45; gD2=0.85; gD3=0.45; gD4=0.50; gF1=gF2=gF3=gF4=0; gKLim=1; gDLim=1; gFLim=0; gE=100; rDispP=rDispN=-0.40; rForceP=rForceN=-1.00; uForceP=uForceN=-0.40. As already highlighted, the number of cyclic out-of-plane experimental tests is very limited. Further experimentation is needed to achieve a more robust and reliable calibration of the hysteretic parameters of the out-of-plane response of unreinforced masonry infills, also characterized by different geometric and mechanical properties.

4 NONLINEAR ANALYSIS PROCEDURE

The nonlinear time-history analyses have been performed by scaling up to the design PGA of each case-study building ten bidirectional ground motions selected in the European Strong Motion (ESM) Database [33]. The selected records were registered on stiff and horizontal soils (i.e., type A soils according to Eurocode 8 [3]). Both components of the selected records were simultaneously matched to the 5%-damped design spectrum at Life Safety Limit State by using wavelets and the RspMatchBi software [34]. The record component registered in the NS direction was applied along the longitudinal global direction, while the component registered in the EW direction was applied along the transverse global direction. Further details on record selection are available in [16].

Nonlinear time-history analyses were performed on the Bare Frame (BF) models, on the infilled frame models with WL infills and SL infills but modelling only their in-plane response (WL and SL models), and on the infilled frame models with WL infills and SL infills with modelling both the out-of-plane response and the in-plane/out-of-plane interaction effects (WLOOP and SLOOP models). In the following, each case-study building is identified using an acronym, such as *X*P*Y*_*Z*, in which *X* is the number of storeys, *Y* the design PGA at Life Safety Limit State expressed in g/100, Z the model identifier (BF, WL, SL, WLOOP, and SLOOP).

Consistently with the design process, a 5% damping ratio was used to calculate damping forces during the analyses. More specifically, mass- and tangent stiffness-proportional Rayleigh damping model was adopted.

5 TIME-HISTORY ANALYSIS RESULTS

In this section, the results of the time-history analyses are presented and discussed. Namely, the outcomes in terms of PFA/PGA profiles and PSA/PFA spectral shapes are shown. The spectral shapes are calculated by assuming a code-consistent value of the damping ratio equal to 5%. For each case-study building, the results shown are obtained as the average of the results obtained from the ten time-history analyses performed under the action of the ten bidirectional ground motions selected. For the sake of brevity, only some significant results are shown. These results can be considered representative of the general trends observed from the outcomes of all the numerical analyses. Then, these outcomes are compared with the results of the application of code and literature proposals previously described.

5.1 PFA/PGA profiles

The PFA/PGA profiles along the longitudinal direction for a selection of case-study buildings are shown in Figure 3.

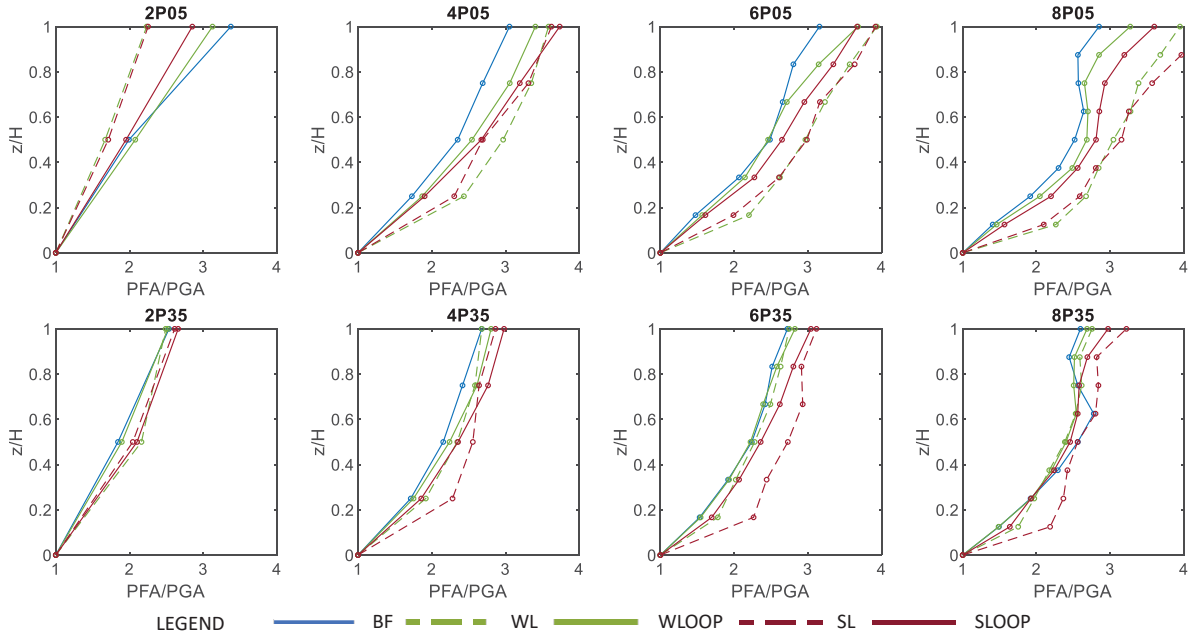

Figure 3: PFA/PGA profile along the longitudinal direction of a selection of case-study buildings.

Some considerations can be drawn:

i. The maximum value of PFA/PGA is generally between 3 and 4, it is registered at top floors and is lower for buildings designed and analyzed for higher PGA (see point v. for comments on this). Among code and literature formulations, NZSEE2017 [5] approach returns a maximum PFA/PGA value equal to 3 at the top floors of buildings; in addition, a maximum PFA/PGA ratio equal to 4 was expected at top storeys according to Uniform Building Code [35]. Hence, the PFA/PGA maximum values obtained from the analyses can be deemed reasonable.

ii. The shape of the profiles is roughly linear for 2-storey buildings, while it becomes multilinear for the other buildings and non-monotonic for taller (6- and 8-storey) buildings. This is an effect of the influence of higher vibration modes, which, as it is well-known, is more significant in high-rise structures. This is expected based on the more refined code and literature proposals discussed in section 2. The effect of higher modes appears also more visible and significant for infilled structures than for bare structures, as well as in presence of higher nonlinearity (i.e., for higher PGA demand).

iii. Generally, at fixed building and at fixed floor, the maximum PFA/PGA value is registered for infilled buildings without modelling of out-of-plane response and in-plane/out-of-plane interaction, except for the 2-storey buildings. This occurs due to the dependence of the PFA on $S_a(T_1)$. In fact, in 4-, 6-, and 8-storey buildings, $S_a(T_1)$ is generally higher for infilled buildings, since T_1 is lower for infilled buildings and T_1 for bare frames is higher than the corner period T_C equal to 0.40 s; on the contrary, T_1 for 2-storey bare structures is lower than T_C, so, infilled buildings, which are always characterized by lower T_1 than bare buildings, are characterized, in this case,

also by lower $S_a(T_1)$. The dependency of the PFA values on $S_a(T)$ is expected based on the more refined code and literature proposals discussed in section 2.

iv. Generally, at fixed building, the PFA/PGA profiles for infilled buildings with out-of-plane response of infills and in-plane/out-of-plane interaction modelled tend to approach the profile obtained for the bare structures. This is expected, since when the in-plane/out-of-plane interaction is modelled, the in-plane response of the infill deteriorates, in terms of both stiffness and strength capacity, due to the out-of-plane displacement demand. So, the general behaviour of the building results intermediate between those of the bare and of the infilled (with in-plane response only of infills modelled) buildings.

v. Generally, the trends described above are confirmed when passing from the buildings designed and analyzed for PGA equal to 0.05 g to those designed and analyzed for PGA equal to 0.35 g. However, they are sometimes disturbed due to structural nonlinearity, which in general, yields to a reduction of the PFA/PGA demand in the case-study buildings. This is expected based on the more refined code and literature proposals discussed in section 2. Note that due to the modelling approach adopted (see section 3.1), the case-study buildings experience nonlinearity (in terms of tangent stiffness variation during the analysis) due to elements'/infills' cracking, while their elements do not yield. In other words, the reduction of PFA at increasing demand PGA and, as will be shown in the following, period elongation and PSA reduction at increasing demand PGA is mainly due to elements'/infills' cracking. This has been observed also by Petrone et al. [10].

Based on the above considerations, which are corroborated by the discussion of literature and code proposals presented in section 2, in can be concluded that, with reference to the set of case-study buildings analyzed for this study, the significant parameters influencing the values of PFA/PGA ratios are the $S_a(T)$ acting on the structure and on the PGA value itself (which is representative of the level of expected nonlinearity in the structure), both referred to the ground motion. On the other hand, the shape of the PFA/PGA profile depends on the importance of higher modes, which is higher for taller buildings than for lower buildings, as well as for infilled buildings than for bare buildings.

5.2 PSA/PFA spectral shapes

The PSA/PFA spectral shapes obtained along the longitudinal direction for a selection of floors of a selection of case-study buildings are shown in Figure 4. The value of T_1 used to normalize the period T_a is the period of the bare frame for WLOOP and SLOOP models: in fact, as previously discussed, due to the in-plane/out-of-plane interaction effects, the behaviour of models in which the out-of-plane response of infills is modelled is intermediate between the behaviour of the bare structural model and that of the infilled structural model with only the in-plane response of infills considered; for bare and WL/SL models, the period adopted for normalization is the one calculated by means of modal analysis of the elastic uncracked model.

Some considerations can be drawn:

i. The maximum value of PSA/PFA is significantly variable from floor to floor, as some of the code and literature models described in section 2 show. In general, it appears dependent on the PFA/PGA value: the higher the PFA/PGA, the higher the maximum value of PSA/PFA. The maximum observed value of the PSA/PFA ratio is roughly equal to 5.5, which is consistent with the maximum value, equal to 5, predicted by the proposal by Petrone et al. [10] adopted also by the Italian code.

ii. The spectral shapes are characterized, in general, by multiple peaks corresponding to the different vibration modes of the structure. This is quite evident in taller buildings, in which the maximum value of PSA/PFA associated with the higher modes (i.e., at T_a/T_1 significantly lower than the unit) may be even higher than that associated with the first vibration mode (i.e., at T_a similar to T_1). In 2-storey buildings, the effect of higher modes is visible only at the first floor, at which, actually, the maximum influence of the second vibration mode is expected. On the other hand, in the 8-storey buildings, peaks of PSA/PGA associated with higher modes are visible at different T_a/T_1 values dependently on the floor considered. This occurs because at bottom floors the predominant effect among higher modes may be associated with different higher modes from floor to floor (e.g., the second or the third vibration mode of the structure).

iii. In general, infilled buildings are characterized by higher values of the maximum PSA/PFA ratio associated with the first vibration mode with respect to bare buildings, except for the 2-storey buildings. This occurs, most likely, because $S_a(T_a=T_1)$ is higher for infilled buildings with respect to $S_a(T_a=T_1)$ for bare buildings, since T_1 of the infilled building is lower than T_1 of the bare building, which, in tune, is higher than T_C. As already explained when discussing maximum PFA/PGA trends, this is not true for 2-storey buildings, since in this case $S_a(T_a=T_1)$ is lower for infilled buildings than for bare buildings. This occurs because T_1 of the infilled building is still lower than T_1 of the bare building, but T_1 of the bare building is lower than T_C. The dependence of the maximum PSA/PFA value on $S_a(T_a=T_1)$ may be also expressed by relating it directly to the period T_1, as done by Petrone et al. [10].

iv. As also shown when discussing the PFA/PGA profiles, also the spectral shapes for infilled buildings with modelling of the out-of-plane response of infills and of the in-plane/out-of-plane interaction effects are intermediate between those obtained for the bare models and those obtained for the infilled models with modelling of the in-plane response only of the infill walls. The fact that for WLOOP and SLOOP models the peak of PSA/PFA due to resonance with the first vibration mode occurs at $T_a/T_1<1$ is due to the fact that, in this case, T_a is normalized with respect to T_1 of the bare frame, while the real resonance period is lower than it, being intermediate between the bare and the infilled structure elastic vibration period.

v. Generally, the trends described above are confirmed when passing from the buildings designed and analyzed for PGA equal to 0.05 g to those designed and analyzed for PGA equal to 0.35 g. However, the peak PSA/PFA associated with the first vibration mode of the structure is noticeably reduced due to the effect of structural nonlinearity; in addition, the resonance period is higher than T_1 for the period elongation due to structural nonlinearity. Remember that, as previously highlighted, this effect is mainly due to elements'/infills' cracking. Both effects of structural nonlinearity are expected also by applying the more refined literature proposals discussed in section 2. Also note that, even if with a lower impact, also the peaks associated with higher vibration modes may be reduced due to structural nonlinearity. This was observed also by Surana et al. [11].

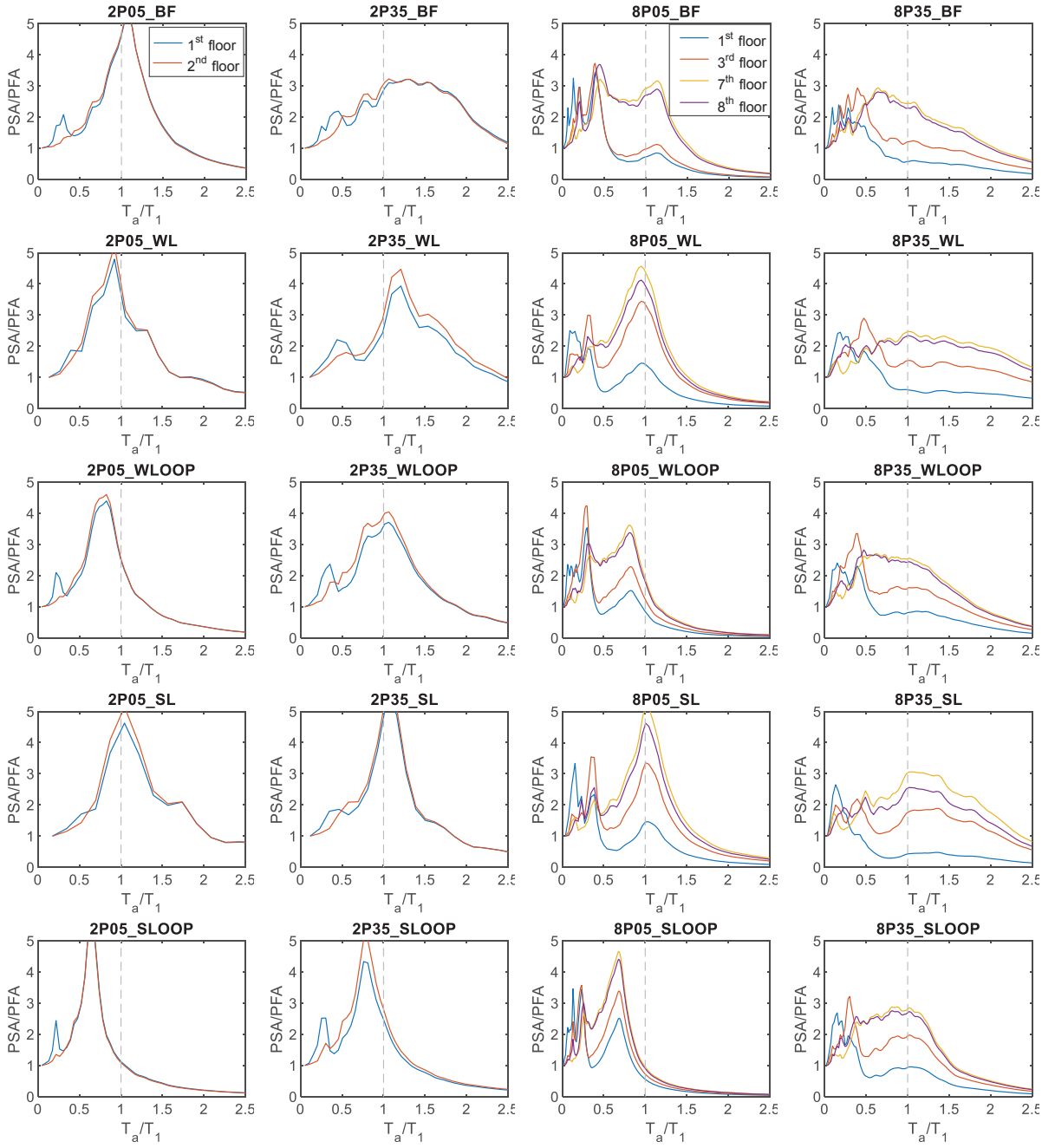

Figure 4: PSA/PFA spectral shapes along the longitudinal direction of a selection of case-study buildings.

Based on the above considerations, which are corroborated by the discussion of literature and code proposals presented in section 2, in can be concluded that, with reference to the set of case-study buildings analyzed for this study, the significant parameters influencing the values of the maximum PSA/PFA ratios associated with the resonance with the i-th vibration mode at a certain floor are the PFA/PGA value at that floor, the $S_a(T_a=T_i)$ value, potentially substituted directly by T_i, and the PGA value (which is representative of the level of expected nonlinearity in the structure). On the other hand, the shape of the PSA/PFA profile is characterized by a peak associated with the resonance with the structure first vibration mode and with a group of close peaks associated with the resonance with the structure higher modes.

6 CONCLUSIONS

- Floor response spectra are a useful tool for the assessment of the seismic demand on non-structural components, whose safety check is a paramount issue in performance-based earthquake engineering. This study was dedicated to the assessment via nonlinear time-history analyses of floor response spectra of case-study reinforced concrete framed structures designed according to Eurocodes for four different levels of design peak ground acceleration at Life Safety Limit State. The case-study bare structures have also been analyzed by including in the model two different kinds of uniformly-distributed infill walls. The main novelty of this study is not only the assessment of floor spectra for infilled reinforced concrete buildings, which has been rarely addressed in the past, but above all the fact that infill walls are modelled by considering their in-plane response, as usual, and their out-of-plane response, as well as the in-plane/out-of-plane interaction, i.e., the degradation of the in-plane response due to the out-of-plane seismic demand and vice-versa.
- Based on literature and code existing formulations, the main parameters which are expected to influence floor response spectra have been identified, namely the floor height normalized with respect to the building height, the pseudo-spectral accelerations acting on the considered building, the vibration periods of the considered building and the shape of its vibration modes, the building height, the expected peak ground acceleration demand. Moreover, floor spectra shape is strongly influenced by higher vibration modes and by the nonlinearity demand experienced by the structure.
- Generally, at fixed building, the PFA/PGA profiles for infilled buildings with out-of-plane response of infills and in-plane/out-of-plane interaction modelled tend to approach the profile obtained for the bare structures. This is expected, since when the in-plane/out-of-plane interaction is modelled, the in-plane response of the infill deteriorates, in terms of both stiffness and strength capacity, due to the out-of-plane displacement demand. So, the general behaviour of the building results intermediate between those of the bare and of the infilled (with in-plane response only of infills modelled) buildings.
- Also the spectral shapes for infilled buildings with modelling of the out-of-plane response of infills and of the in-plane/out-of-plane interaction effects are intermediate between those obtained for the bare models and those obtained for the infilled models with modelling of the in-plane response only of the infill walls.
- Based on the above discussion, formulations for the assessment of floor response spectra have will be proposed for both bare and infilled buildings in future studies.

ACKNOWLEDGMENTS

This work was developed under the financial support of ReLUIS-DPC 2019-2021 funded by the Italian Department of Civil Protection (DPC). This support is gratefully acknowledged.

REFERENCES

[1] M.E. Rodriguez, J.I. Restrepo, A.J. Carr, Earthquake-induced floor horizontal accelerations in buildings. *Earthquake Engineering and Structural Dynamics* 200, **31**, 693-718, 2002.

[2] V. Vukobratović. *The influence of nonlinear seismic response of structures on the floor acceleration spectra*. Doctoral thesis, University of Ljubljana, Faculty of Civil and Geodetic Engineering, Ljubljana, Slovenia, 2015.

[3] CEN, *Eurocode 8. Design of structures for Earthquake Resistance. Part 1-1: General Rules, Seismic Actions and Rules for Buildings*. Brussels, 2004.

[4] ASCE/SEI 7-10, *Minimum Design Loads for Buildings and Other Structures*. ASCE 7-10. Reston, VA: ASCE, 2010.

[5] New Zealand Society for Earthquake Engineering (NZSEE), Structural Engineering Society New Zealand Inc. (SESOC), New Zealand Geotechnical Society Inc., Ministry of Business, Innovation and Employment, Earthquake Commission, *The Seismic Assessment of Existing Buildings (the Guidelines), Part C – Detailed Seismic Assessment*, 2017.

[6] New Zealand Society for Earthquake Engineering (NZSEE), *NZS 1170.5:2004. Structural design actions. Earthquake design Actions*, 2004.

[7] Ministero delle Infrastrutture e dei Trasporti, *Circolare esplicativa delle Norme Tecniche per le Costruzioni*. Supplemento ordinario n. 5 Gazzetta Ufficiale 11 febbraio 2019. (in Italian).

[8] Ministero delle Infrastrutture e dei Trasporti, *Decreto ministeriale 17 gennaio 2018 - Norme Tecniche per le Costruzioni*. Supplemento ordinario n. 42 Gazzetta Ufficiale 20 febbraio 2018. (in Italian).

[9] A.K. Chopra. *Dynamics of Structures, 5th edition*, Pearson, London, United Kingdom, 2017.

[10] C. Petrone, G. Magliulo, G. Manfredi, Seismic demand on light acceleration-sensitive nonstructural components in European reinforced concrete buildings. *Earthquake Engineering and Structural Dynamics*, **44**, 1203-1217, 2015.

[11] M. Surana, M. Pisode, Y. Singh, D.H. Lang, Effect of URM infills on inelastic floor response of RC frame buildings. *Engineering Structures*, **175**, 861-878, 2018.

[12] P.M. Calvi, T.J. Sullivan, Estimating floor spectra in multiple degree of freedom systems. *Earthquakes and Structures*, **7**(1), 17-38, 2014.

[13] V. Vukobratović, P. Fajfar, A method for the direct estimation of floor acceleration spectra for elastic and inelastic MDOF structures. *Earthquake Engineering and Structural Dynamics*, **45**, 2495–2511, 2016.

[14] V. Vukobratović, P. Fajfar, Code-oriented floor acceleration spectra for building structures. *Bulletin of Earthquake Engineering*, **15**(7), 3013-3026, 2017.

[15] CEN, *Eurocode 2. Design of Concrete Structures. Part 1-1: General Rules and Rules for Buildings*. Brussels, 2004.

[16] M. Di Domenico, *Out-of-plane seismic response and modelling of unreinforced masonry infills*. PhD Dissertation. University of Naples Federico II, Naples, Italy, 2018.

[17] P. Ricci, M. Di Domenico, G.M. Verderame, Effects of the in-plane/out-of-plane interaction in URM infills on the seismic performance of RC buildings designed to Eurocodes. *Journal of Earthquake Engineering*, 2020. doi: 10.1080/13632469.2020.1733137.

[18] F. McKenna, G.L. Fenves, M.H. Scott, OpenSees: *Open System for Earthquake Engineering Simulation*. Pacific Earthquake Engineering Research Center. University of California, Berkeley, CA, USA, 2004.

[19] C.B. Haselton, A.B. Liel, S. Taylor-Lange, G.G. Deierlein, *Beam-column element model calibrated for predicting flexural response leading to global collapse of RC frame buildings*. PEER Report No. 2007/03. Pacific Earthquake Engineering Research Center, University of California, Berkeley, CA, USA, 2008.

[20] M.N. Fardis, A. Papailia, G. Tsionis, Seismic fragility of RC framed and wall-frame buildings designed to the EN-Eurocodes. *Bulletin of Earthquake Engineering*, **10**(6), 1767-1793, 2012.

[21] G.M. Calvi, D. Bolognini, Seismic response of reinforced concrete frames infilled with weakly reinforced masonry panels. *Journal of Earthquake Engineering*, **5**(2), 153-185, 2001.

[22] G. Guidi, F. da Porto, M. Dalla Benetta, N. Verlato, C. Modena, Comportamento sperimentale nel piano e fuori piano di tamponamenti in muratura armata e rinforzata. *Proceedings of the XV ANIDIS, L'Ingegneria Sismica in Italia*, Padua, Italy, 2013. (in Italian).

[23] T.B. Panagiotakos, M.N. Fardis, Seismic response of infilled RC frames structures. *11th World Conference on Earthquake Engineering*. June 23-28, Acapulco, México, 1996.

[24] M.N. Fardis (editor). *Experimental and numerical investigations on the seismic response of RC infilled frames and recommendations for code provisions*. *ECOEST/PREC8 Report No.6*. Laboratorio Nacional de Engenharia Civil Publications, Lisbon, 1996.

[25] P. Ricci, M. Di Domenico, G.M. Verderame. Empirical-based out-of-plane URM infill wall model accounting for the interaction with in-plane demand. Earthquake Engineering and Structural Dynamics, **47**(3), 802-827, 2018.

[26] M.T. De Risi, M. Di Domenico, P. Ricci, G.M. Verderame, G. Manfredi, Experimental investigation on the influence of the aspect ratio on the in-plane/out-of-plane interaction for masonry infills in RC frames. *Engineering Structures*, **189**, 523-540, 2019.

[27] M. Di Domenico, M.T. De Risi, P. Ricci, G.M. Verderame, G. Manfredi, Empirical prediction of the in-plane/out-of-plane interaction effects in clay brick unreinforced masonry infill walls. *Engineering Structures*, **227**, 2021.

[28] R. Angel, D.P. Abrams, D. Shapiro, J. Uzarski, M. Webster, *Behaviour of reinforced concrete frames with masonry infills*. University of Illinois Engineering Experiment Station. College of Engineering. University of Illinois at Urbana-Champaign, 1994.

[29] M. Di Domenico, P. Ricci, G.M. Verderame, Experimental assessment of the influence of boundary conditions on the out-of-plane response of unreinforced masonry infill walls. Journal of Earthquake Engineering, **24**(6), 881-919, 2020.

[30] L.N. Lowes, N. Mitra, A. Altoontash, *A beam-column joint model for simulating the earthquake response of reinforced concrete frames*. PEER Report No. 2003/10. Pacific Earthquake Engineering Research Center, University of California, Berkeley, CA, USA, 2004.

[31] M. Di Domenico, P. Ricci, G.M. Verderame, Experimental assessment of the out-of-plane strength of URM infill walls with different slenderness and boundary conditions. *Bulletin of Earthquake Engineering*, **17**(7), 3959-3993, 2019.

[32] A. Furtado, H. Rodrigues, A. Arêde, H. Varum, Experimental evaluation of out-of-plane capacity of masonry infill walls. *Engineering Structures*, **111**, 48-63, 2016.

[33] L. Luzi, R. Puglia, E. Russo & ORFEUS WG5, *Engineering Strong Motion Database, version 1.0*. Istituto Nazionale di Geofisica e Vulcanologia, Observatories & Research Facilities for European Seismology, 2016.

[34] D.N. Grant, Response spectral matching of two horizontal ground-motion components. *Journal of Structural Engineering*, **137**(3), 289-297, 2010.

[35] International Conference of Building Officials, *Uniform Building Code*. Whittier, CA, USA, 1997.